Universal Multifractal Scaling of Synthetic Aperture Radar Images of Sea-Ice

Tony Falco, Frédéric Francis, Shaun Lovejoy, Daniel Schertzer, Bryan Kerman, and Mark Drinkwater

Abstract— **Multifrequency, multipolarization imaging radar scattering coefficient data sets, acquired by synthetic aperture radar (SAR) over sea-ice, were studied in order to reveal their scale-invariant properties. Two distinct scenes were acquired at C-band (5.6 cm) and L-band (25 cm) wavelengths for three different linear polarizations (HH, VV, and HV). These sea-ice radar scattering coefficient fields were investigated by applying both Fourier and multifractal analysis techniques. The (multi) scaling of the data is clearly exhibited in both scenes for all three polarizations at L-band and for the HV polarization at C-band. The fields presenting this symmetry were found to be well described by universal multifractals. The corresponding parameters α, C_1, and H were determined for all these fields and were found to vary little with only the parameter H (characterizing the degree of nonconservation) displaying some systematic sensitivity to polarization. The values found for the universal multifractal parameters are $\alpha \approx 1.85 \pm 0.05$, $C_1 \approx 0.0086 \pm 0.0041$, and $H \approx -0.15 \pm 0.05$.**

I. INTRODUCTION

SEA-ICE fields, like the product of many other nonlinear dynamical geophysical processes, is characterized by extreme variability over a wide range of scales. Since it is clear that the inhomogeneity extends down to millimetric scales, remote measurements of its properties (typically performed at much larger scales) will depend critically on this variability. For synthetic aperture radar sea-ice data, the highly variable scattering coefficient fields will depend on the basic dynamical and morphological parameters: thickness, density, salinity and temperature. While standard modeling and analysis methods can at best handle this variability over narrow ranges of scale, multifractal theory exploits the scaling symmetries present in geophysical fields in order to quantify their variability over arbitrarily large ranges. In fact, multifractal analysis has been successfully applied to investigate geophysical fields such as rainfall and cloud fields [1]–[4], ocean surface [5]–[7], wind turbulence [8], [9], topography [10], [11], earthquakes [12], and temperature fields [9]. An introductory discussion and overview of multifractals and the related analysis techniques for remote sensing may be found in [13] and [14] (see also [5]).

Research has shown that geometric sets associated with sea-ice structures [15] and sea-ice keels [16], [17], are fractal and multifractal which suggests that the underlying dynamical fields are multifractal. While these studies were concerned solely with demonstrating the scaling behavior of geometric sets associated with sea-ice, this work will demonstrate and quantify the multiscaling symmetries present in the sea-ice radar scattering coefficient field.

II. DATA AND ANALYSIS

The data studied here consist of two distinct sea-ice SAR scattering coefficient scenes each having 512 × 512 pixel elements with 12.5 m resolution. Both scenes were taken by the Jet Propulsion Laboratory (JPL) airborne SAR (AIRSAR) which operates simultaneously at the C-band (5.6 cm) and L-band (25 cm) wavelength ranges [18], transmitting and receiving from separate antennas in three linear polarization combinations namely HH, VV, and HV where the symbols represent horizontal (H) and vertical (V) polarization in the transmitted and received beams, respectively. The SAR backscatter images were taken from an altitude of 9 km over a section of the Beaufort Sea located at 76° north latitude and 165° west longitude during March 1988 [19]. Two of these sea-ice SAR backscatter amplitude fields are shown below in Fig. 1.

C-band backscattering relates mostly to the micro-physical properties of the medium via the dynamic-thermodynamic relations of the sea-ice. For instance, how the distribution of brine and gas bubbles in sea-ice drives the dynamic strength of the sea-ice also controls the dielectric tensor within the ice, and thereby determines the scaling of the scattering amplitude fields. The L-band shows a somewhat different set of relations responding to bulk properties of the ice and characteristics of the sea-ice determined by ice dynamics; such as morphology, the stress-strain field, and the general salinity or roughness characteristics. Due to their different thermodynamic histories, the characteristics of the amplitude field itself are different for old and young ice. Finally, the HH and VV polarizations are mostly sensitive to the surface characteristics whereas the HV polarizations to those of the internal properties. Further, more detailed information on polarimetric scattering signatures of sea-ice can be found in [20] and [41].

III. FOURIER POWER SPECTRA AND SCALING

If the dynamical processes which give rise to the ice fields are scaling, then surface topography, salinity, and temperature

(a)   (b)
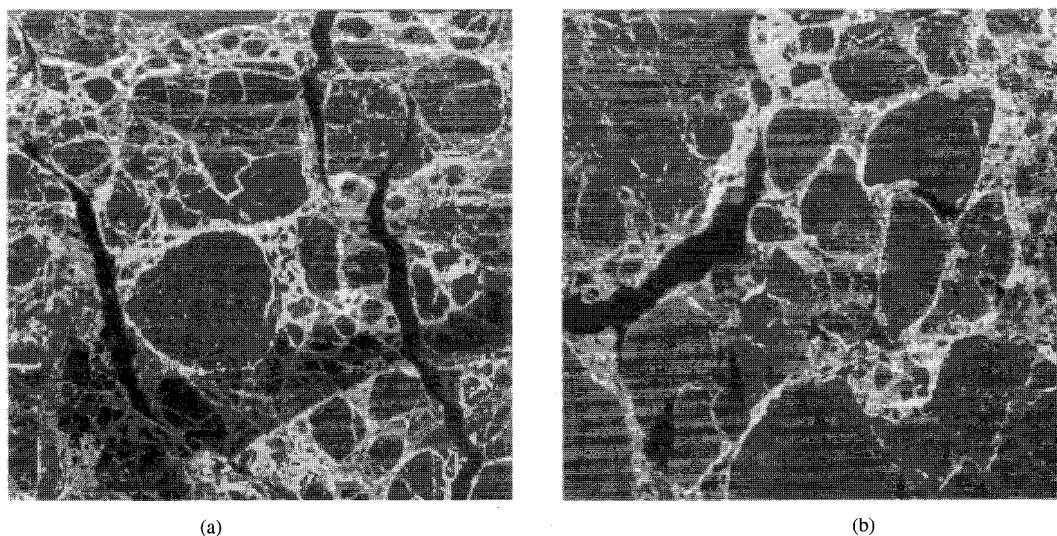
Fig. 1.   Two distinct SAR sea-ice scattering coefficient fields taken over the Beaufort Sea at HV polarization. (a) C-band (Scene 1). (b) L-band (Scene 2).

fields will also be scaling; so will the resulting dielectric tensor at microwave frequencies. Its variability will have no characteristic length except that associated with the wavelength under consideration. When such a surface is observed by radar, the scattered intensity is a spatial average (over the pulse volume) of the reflected wave weighted by a phase term which depends on the position of the scattering element and the wavevector of the radar. Mathematically, the observed signal will be a Fourier component of the radar cross-section field. When the latter is scaling, we seek the Fourier component of the corresponding multifractal field. A very similar problem has recently been studied by [21]; that of radar measurements of rain. Each drop is nearly spherical, and a scalar wave approximation is quite accurate. With the help of Lie cascades [39] (which allow for a vector or tensor multifractal representation), Duncan was able to find a general solution to the scalar multifractal radar observer's problem. In particular, he argued that there were only two fundamental differences between the statistical properties of the radar reflectivities and the (scalar) radar cross section. The first is the introduction of a fundamental scale corresponding to the pulse volume, and the second, the existence of a systematic scaling bias in the statistics. Note that these results concern the statistics and do not imply that the "speckle" effect discussed here can be removed on an echo by echo basis. In terms of the basic (universal) multifractal exponents discussed below (α, C_1), Duncan's results imply that they will be unaffected (i.e., we will obtain the same α, C_1 for the radar cross-section and for the radar scattering amplitude fields). Recently [42] more precise results have been obtained (including a multifractal explanation for "speckle").

While the generalization of Duncan's results to the full multifractal tensor problem necessary for studying sea-ice is a subject for future study, we anticipate that the various polarized returns of such a surface will also be multifractal down to the footprint (pulse volume) scale. However, before proceeding with a multifractal analysis of the reflectivities, we must verify the basic scaling symmetry in this radar scattering

coefficient field. For fields which are roughly statistically isotropic, a sensitive and straightforward means to do this is to estimate the standard (isotropic) power spectrum of the data [$E(k)$ at wavenumber k], defined by the ensemble average of the squared modulus of Fourier transform of the data followed by an angular integration which yields the standard spectral energy $E(k)$. For an isotropic scale invariant field (i.e., it is self-similar), $E(k)$ will be a power law

$$E(k) \propto k^{-\beta} \tag{1}$$

where the spectral exponent β is estimated from the slope of a double logarithm plot of $E(k)$; recall that $k = 1$ corresponds to 512×12.5 m $= 6.4$ km.

While the energy spectrum is defined as an ensemble average, the estimates presented here are from single samples—which we treat as single realizations of a stochastic multifractal process. In order to reduce spectral leakage, a Hanning window was used, and since single samples were used, we in fact calculated the corresponding modified periodogram. Since the scaling itself is a statistical symmetry (necessarily broken on every single realization; it only holds exactly on ensemble averages), we therefore expect nonnegligible random deviations around the power law due to the chance presence (or absence) of high-order singularities. In addition, in multifractals, the variance (as well as the other moments) varies as a systematic power law function of resolution [with exponent $K(2)$; (4), studied below], hence we are interested instead in the spectral exponent β, rather than the spectrum itself. Therefore no special variance reduction techniques were used [22], [27].

In addition to (occasionally large) random deviations from power law form due to inadequate sample size, we anticipate some systematic deviation from power laws due to the anisotropy of the field.[1] Although a thorough discussion of

[1] We discuss the anisotropy of the spatial field at fixed look angle and fixed polarization, not the anisotropy at a given location as a function of look-angle or polarization, [41].

TABLE I
COMPILATION OF RESULTS. THE VALUES OF α AND C_1 ARE AVERAGES
OVER THE ESTIMATES OBTAINED WITH $q = 0.5$, 1.5, AND 2.0

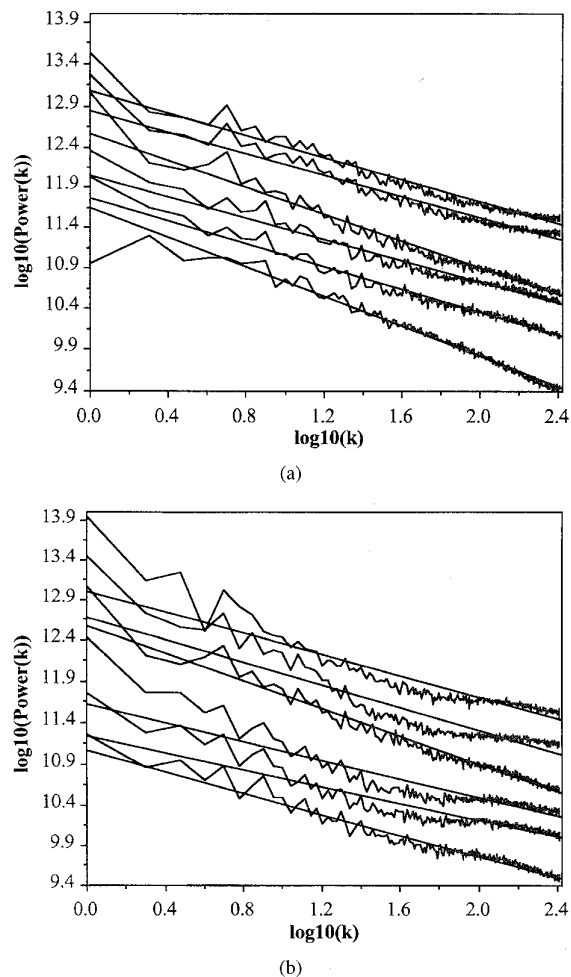| Scene 1				
L-Band				
Polarization	α	C_1	H	β
HH	1.81	0.0096	-0.16	0.66
HV	1.80	0.0095	-0.16	0.66
VV	1.82	0.0087	-0.15	0.68
C-Band				
Polarization	α	C_1	H	β
HH	1.85	0.0070	-0.15	0.68
HV	1.80	0.011	-0.08	0.83
VV	1.85	0.0072	-0.15	0.69
Scene 2				
L-Band				
Polarization	α	C_1	H	β·
HH	1.97	0.0059	-0.14	0.71
HV	1.93	0.019	-0.03	0.91
VV	1.95	0.0055	-0.17	0.65
C-Band				
Polarization	α	C_1	H	β
HH	1.81	0.0039	-0.23	0.51
HV	1.88	0.012	-0.17	0.65
VV	1.84	0.0045	-0.21	0.56

(a)

(b)

Fig. 2. (a) Power spectra showing the well-respected scaling, especially linear in the HV polarization for both scenes in their L-band data (from top to bottom, the curves are HH, VV, and HV for scene 1 followed by HH, VV, and HV for scene 2). The curves were offset by 0.5 in the vertical so as to avoid overlap. (b) Power spectra showing the well-respected scaling, especially linear in the HV polarization for both scenes in their C-band data (from top to bottom, the curves are HH, VV, and HV for scene 1 followed by HH, VV, and HV for scene 2). The curves were offset by 0.5 in the vertical so as to avoid overlap.

anisotropy is outside of our present scope (it is the subject of a paper in preparation) we give a quick summary here. Geophysical fields such as sea-ice are rarely if ever isotropic, however their anisotropy by no means implies breaks in their scaling. The framework for treating scaling anisotropy is "Generalized Scale Invariance" [1], [23], [24] and involves a group of scale changing operators which define an exponent called the generator. Isotropic scaling corresponding to self-similar fractals and multifractals have generators which are identity operators; in the anisotropic case, the generator will generally be a nonlinear (even random) function. Work in progress approximates the generator by a matrix ("linear GSI") and thus confirms and quantifies the anisotropic scaling displayed in sea-ice, particularly the strong anisotropy associated with fractures, shears and ridges.

Thus in principle, anisotropic generalizations of the power spectrum are necessary (see [25]); without these, one might for example expect oscillations periodic in log wavenumber. However, since the angle integration is quite effective at averaging out spectral anisotropy, only very severe anisotropy will lead to a significant effect in the usual angle averaged (isotropic) spectrum. We directly verified from the full 2-D spectrum that this was indeed the case (we estimated the linear approximation to the generators using the scale invariant generator technique of [26]: results will be reported elsewhere). Note that following this, in the rest of this paper, only isotropic analysis techniques (such as square averaging boxes at all scales) are used.

With these caveats about possible deviations from pure power law behavior—even with perfectly scaling ice dynamics—Fig. 2(a) shows that, over the entire accessible range, the scaling is reasonably well respected for all

polarizations of the L-band data from both scenes with the spectral exponent showing some variation. Estimates of β are given in Table I. The corresponding analysis for the C-band data yields somewhat less satisfying results [Fig. 2(b)]. Once again, the scaling relation holds for the HV polarization as seen in Fig. 2(a). It would be nice to be able to use rigorous statistical goodness of fit testing procedures to quantify the statement that the scaling is "reasonably well respected." However, even for the theoretically simpler monofractal processes (such as fractional Brownian motion where β can be related to a fractal dimension), such tests do not exist (see however [27] for some numerics). Here, the statement is based on comparing spectra from multifractal simulations with measured parameters with the data, and noting that deviations of similar magnitude are typically obtained.

However, if we now consider the high wavenumbers corresponding to distances less than approximately 50 m, the spectra of both scenes at the HH and VV polarization scattering coefficient fields deviate slightly from the expected straight line behavior. Since there are no known physical properties of sea-ice that correspond to a phenomena occurring at a fundamental length scale of around 50 m and the L-band spectrum indicates that scaling is apparently respected at that scale, we suspect that this deviation for the C-band HH and VV polarization scattering coefficient data results from an artifact introduced during the complex data acquisition and preprocessing analysis stages in the C-band data.

IV. MULTIFRACTAL ANALYSIS: THEORY AND SAMPLE RESULTS

The above analysis demonstrates that the radar backscatter amplitude of these sea-ice SAR images is scaling over the observed range 12.5 m to 6.4 km. We will now show that the field in fact exhibits multiple scaling; β being only a single member of an infinite hierarchy of exponents. As already mentioned, whereas scale invariant geometric sets are fractals, scale invariant fields (and dynamical processes) will be multifractals. This implies that each element in a multifractal is assigned not only a set of coordinates but also an intensity. The focus is thus shifted from examining how sea-ice geometries vary with scale to determining the functional relationship between the SAR sea-ice scattered intensity distribution and the scale at which the field is observed.

Let us first define what is meant by the scattering coefficient at a given scale. For roughly isotropic fields, this is achieved most easily by superimposing an $l \times l$ pixel size square grid onto this field. Denoting the scale of the entire scene by L (= 512 pixels = 6.4 km), we thus define the scale ratio, $\lambda = L/l > 1$. The maximum available scale ratio is written as Λ and indicates the field's finest resolution. A scattering coefficient at scale ratio λ, denoted by Z_λ, can be calculated by taking the average of all the intensities of the pixels which fall inside a box (B_λ) of size $l = L/\lambda$ (= 1 pixel = 12.5 m):

$$Z_\lambda = \frac{\int_{B_\lambda} Z_\Lambda d^D \underline{x}}{\int_{B_\lambda} d^D \underline{x}}. \qquad (2a)$$

We can define the order of singularity γ for a multifractal field Z_λ (here representing the radar scattering coefficient) by

$$Z_\lambda \propto \lambda^\gamma \qquad (2b)$$

and a "codimension function" $c(\gamma)$ by [23]

$$\Pr\left(Z_\lambda \geq \lambda^\gamma\right) \propto \lambda^{-c(\gamma)} \qquad (3)$$

where Pr indicates "probability." Equation (3) defines the codimension function $c(\gamma)$ which characterizes the fraction of the probability space filled by singularities of order γ. When $c(\gamma)$ is less than the dimension of the embedding space (D), a geometric interpretation is possible: $D(\gamma) = D - c(\gamma)$ is the fractal dimension of the regions where the

scattering coefficient exceeds λ^γ. Since $c(\gamma)$ describes how the probability distribution varies with resolution, an equivalent picture can be obtained by considering how the qth statistical moments of a field vary with resolution λ:

$$\langle Z_\lambda^q \rangle \propto \lambda^{K(q)} \qquad (4)$$

where "$\langle \, \rangle$" indicates statistical (ensemble) averaging. Equation (4) defines another scaling exponent $K(q)$ called the moment scaling function which is related to $c(\gamma)$ through a Legendre transformation [28]. $K(q)$ determines how the qth statistical moment of the field varies as a function of resolution whereas $c(\gamma)$ determines how the histogram varies with resolution. In order to apply (4) to the data sets to show that the data is multiscaling, we use a generalization of partition function methods to stochastic processes called "Trace Moments" [23]. These arise from averaging moments over all disjoint resolution λ boxes (windows), and then over all the available realizations. The slopes of the log of $\langle Z_\lambda^q \rangle$ estimated this way versus log $[\lambda]$ (Fig. 3) provides an estimate of $K(q)$. Not only are the points in Fig. 3 quite linear (showing the scaling; compare with the straight regression lines) but their slope systematically varies with the order of the moment q. Fig. 4 shows $K(q)$ indicating that this variation is nonlinear, hence the field is multiscaling, multifractal. In comparison, monofractal processes such as Brownian motion and its generalizations would lead to a linear $K(q)$.

Many of the multifractal analysis techniques such as the trace moment only give good estimates of the scaling exponents when they are applied to conservative fields (i.e., they are the direct outcome of multiplicative processes). Actually, (fractional) derivatives (but not integrals) with respect to a conserved field will also yield the same results. Although fractional differentiation (i.e., a Fourier power law filter) is preferable (see e.g., [9]), the (finite) gradient and the (finite) difference) Laplacian of the field are usually sufficient [11]. We confirm here that the exponents $K(q)$ are indeed insensitive to varying orders of differentiation. In Section VI, we directly estimate the order of (fractional) integration[2] (H) needed to yield the observed field from a conservative field finding $H < 0$ corresponding to differentiation.

V. MULTIFRACTAL UNIVERSALITY CLASSES

Since the multiscaling relations in (2)–(4) are general, they do not provide a very satisfactory characterization of Z_λ as it involves an entire (unknown) function $c(\gamma)$, or $K(q)$, which is equivalent to having to determine and represent an infinite number of parameters. However, by considering how a conserved dynamical flux is nonlinearly multiplicatively modulated scale by scale, it has been shown [23], [24], [29] that multifractal processes possess stable and attractive generators. This result is the multiplicative analog of the usual central limit theorem for the addition of random variables. This means that independent of many of the dynamical details of

[2] Because fractional integration corresponds to a power law filter, nonconservative multifractal fields with $H > 0$ will display features of nonstationarity (such as low frequency excess, *tendencies* toward ultraviolent violent catastrophes, etc.) in spite of the fact that within the scaling range they are perfectly stationary (i.e., statistically, translationally invariant).
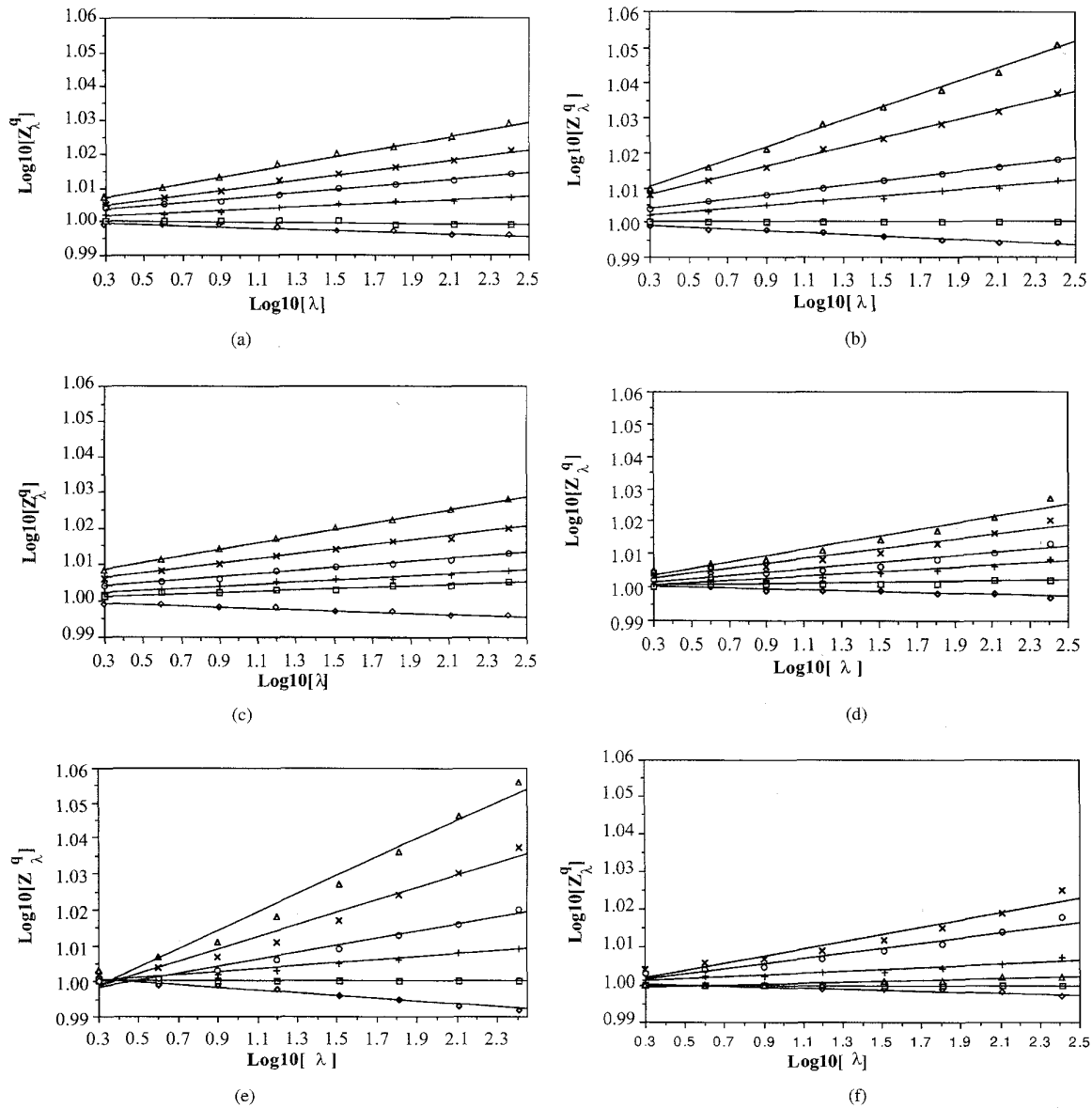
Fig. 3. Scaling curves from the Trace Moment function with q values 2.0, 1.7, 1.4, 1.0, 0.7, and 0.4 from top to bottom for all polarizations of the C-band from scene 1 [(a) HH, (b) HV, and (c) VV polarizations], and of L-band from scene 2 [(d) HH, (e) HV, and (f) VV polarizations].

the process under study, that an overall universal multifractal behavior may be recovered with a dependence upon only three parameters (see however the recent debate about weak versus strong multifractal universality in [30]). Such a representation in terms of universality classes of the conserved process is described by the fundamental parameters α and C_1

$$K(q) = \begin{cases} \left(\dfrac{C_1}{\alpha - 1}\right)(q^\alpha - q) & \forall \quad \alpha \neq 1 \\ C_1 q \log q & \text{for } \alpha = 1 \end{cases} \tag{5}$$

for $0 \leq \alpha \leq 2$. The Lévy index α is a direct measure of the degree of multifractality ([23], [29], [31], [32]). Equation (5) is only valid for $q \geq 0$ when $\alpha < 2$. The case $\alpha = 0$ corresponds to the monofractal extreme, while $\alpha = 2$ is associated with the lognormal multifractal. $0 \leq C_1 \leq D$ is the

codimension of the mean singularity and D is the dimension of the embedding space (equal to $D = 2$ here). If $C_1 > D$, the process will be degenerate on that space [23]; each realization will almost surely be zero everywhere. Since the $\alpha = 2$ case has (nearly) lognormal probability distributions,[3] universal multifractals are compatible with the widespread geophysical phenomenology of lognormal distributions. Note that we have already mentioned the third parameter H; the degree of fractional integration ($H > 0$) (differentiation, $H < 0$) with respect to the conserved multifractal process.

In order to test the universality hypothesis, we use generalization of the trace moments based on Z_Λ^η fields rather

[3] The "bare" Z_λ field [which obeys (5) exactly for all q] will be exactly lognormal, but the observed "dressed" Z_λ field will only obey (5) for $q < q_D$, and when $\alpha = 2$, hence be only approximately log-normal, see below.

than Z_Λ. This "double trace moment" (DTM) technique [11], [33] yields the exponent function $K(q, \eta)$ based on a similar relationship to (4), i.e.,

$$\langle \phi_\lambda^q \rangle \propto \lambda^{K(q, \eta)} \quad \text{where } \phi_\lambda \equiv (Z_\Lambda^\eta)_\lambda \qquad (6a)$$

the new field ϕ_λ is the obtained by degrading the resolution of the ηth power of the finest resolution scattering coefficient Z_Λ^η by spatially averaging it over boxes of scale λ:

$$\phi_\lambda = \frac{\displaystyle\int_{B_\lambda} Z_\Lambda^\eta d^D \underline{x}}{\displaystyle\int_{B_\lambda} d^D \underline{x}}. \qquad (6b)$$

This new exponent $K(q, \eta)$ is related to the previous moment scaling moment function by $K(q, 1) = K(q)$ and

$$K(q, \eta) = K(q\eta, 1) - qK(\eta, 1). \qquad (7)$$

The term $K(q\eta, 1)$ arises because we take the η then q power, whereas the $qK(\eta, 1)$ term is a consequence of the normalization imposed by the spatial averaging over scale λ. For universal multifractals (7) reduces to

$$K(q, \eta) = \eta^\alpha K(q, 1)$$
$$\log K(q, \eta) = \alpha \log \eta + \log K(q, 1) \qquad (8)$$

[as can be seen by plugging (5) into (7)]. Therefore, we can readily test the hypothesis that the scattering coefficient fields belong to multifractal universality classes by testing for a linear region of a plot between $\log[K(q, \eta)]$ versus $\log[\eta]$ for a fixed q; the slope is α. Since the value of α is independent of the initial value of q, the analysis is repeated for various q-values in order to insure that universality is respected and to obtain more reliable estimates of α. This procedure is illustrated in Fig. 5 for two values of q: 0.5 and 1.5. It can be seen that a wide linear region exists which suggests the existence of multifractal universality classes. Both plots have nearly the same slope, $\alpha \approx 1.85$. From the intercepts, together with α and q, we find $C_1 \approx 0.0086$.

As can be seen in Fig. 5, the DTM graphs deviate from the expected straight line behavior at the low and high ends of the $\log[\eta]$ range. Only the linear section of these $\log[K(q, \eta)]$ versus $\log[\eta]$ plots was used to estimate α and C_1. These qualitative changes in the curve are theoretically expected. At the low η end (corresponding to exponents smaller than the very low value $\approx 10^{-3}$), the behavior, is dominated by the weakest values in the field and the break from linearity is likely caused by a low level of space filling noise.

The high η break is more interesting and corresponds to qualitative change for the violent (extreme) fluctuations. Since there is a formal analogy between thermodynamics and multifractals, with $K(q)$ playing the role of a "Massieu" potential, this qualitative change in the behavior is called a "multifractal phase transition" [34]–[36], [40]. What we are
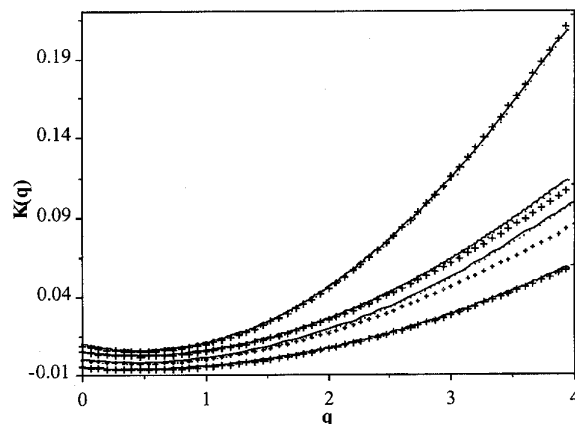

Fig. 4. Empirically determined Moment Scaling functions (using $\alpha = 1.85$, $C_1 = 0.01$), for the HV polarization (from top to bottom) of C-band and scene 1, C-band and scene 2, L-band and scene 1, and L-band and scene 2. Each line is the best fit using the α and C_1 parameters obtained from the DTM. Each curve is offset by 0.01 for clarity of presentation.

examining is a single realization of the sea-ice process, while (6) involves an expectation over the entire infinite ensemble of realizations. Intensities with extremely high values are only rarely encountered in a single sample. This leads to an underestimation of the higher moments of the field. Specifically, for single realizations, discontinuities in the second derivative (second order phase transitions) of $K(q, \eta)$ will occur for [36]:

$$\eta_s \approx \frac{1}{q}\left(\frac{D}{C_1}\right)^{1/\alpha}. \qquad (9)$$

For example, using the values, $D = 2$, $C_1 \approx 0.01$, $\alpha \approx 1.85$, $q = 1.5$ (corresponding to one of the values used in Fig. 5), we find $\eta_s \approx 8$–11, which is roughly the value corresponding to the departure from linearity in Fig. 5. An additional verification of the universal multifractal parameters can be made using the definition of the moment scaling function, (4), and its universal form, (5). The moment scaling function is computed from the first of these two relations over a given range of q-values then it is compared to its *theoretical* form (5) using estimated values for α and C_1 from Table I. The comparison shown in Fig. 4 indicates generally good agreement; at least up to the fourth moment or so.

As of yet, no mention has been made on how to determine the errors on the α and C_1 parameters. Both the moment scaling and DTM algorithms used here give estimates of the errors using the standard least squares fit technique when they calculate the slopes of their respective scaling graphs. However, given the excellent multiscaling observed here [and power law $K(q, \eta)$ versus η curves], it is plausible that larger errors perhaps as large as (± 0.1 in α, ± 0.005 in C_1) are likely to arise purely because of realization to realization variations (see [33] for Monte Carlo studies of this problem). Improved estimates should be obtained using a large number of scenes. At this stage however, the focus is put on i) establishing that sea-ice SAR scattering amplitude fields possess an underlying scaling symmetry which is well described by universal
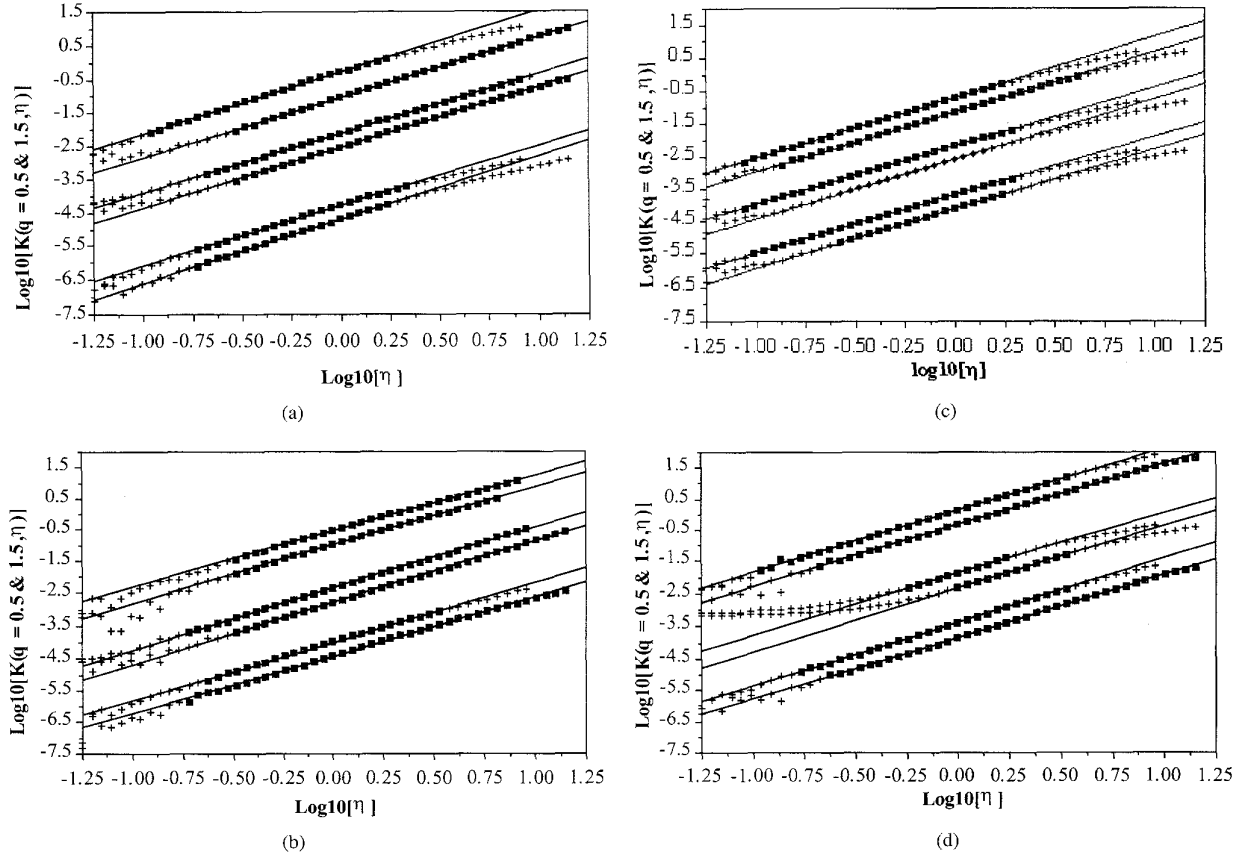
Fig. 5.   Results from the DTM technique with $q = 0.5$ and 1.5 (in pairs) for all the polarizations of the C-band data from (a) scene 1 . (b) Scene 2, and L-band data from (c) scene 1. (d) Scene 2 (HH, HV, VV from top to bottom in each figure).

multifractals; and ii) on investigating the possible dependence of their multifractal parameters of the underlying process on wavelength and polarization used to acquire the data.

VI. NONCONSERVED PROCESS AND THE THIRD UNIVERSALITY PARAMETER H

We have mentioned that the multifractality arises because the nonlinear dynamics are scaling but nevertheless conserve the flux of some basic physical quantity from scale to scale. Since we lack a proper theory of all the dynamics present in sea-ice scattering coefficient (see [37]), we do not know what the proper conserved quantity is. However a priori, there is no reason to suppose that it coincides exactly with the observed scattering amplitude field. Until now, this point was not crucial since the trace moment techniques used to estimate $K(q)$ and $K(q, \eta)$ are unaffected by this conservation property (as long as the process is conservative or a derivative of a conserved process—see [11] for discussion). In order to fully describe the sea-ice SAR scattering amplitude using universal multifractal fields, we therefore require the third universal multifractal parameter which determines the degree of nonconservation of the process H. This parameter quantifies how much the observed field differs from the corresponding conserved process; specifically, the order of fractional integration $(H > 0)$ or differentiation $(H < 0)$ that is needed to obtain a conservative field from a nonconservative one. Since a spectral exponent

is a second-order moment [43], the spectral exponent of the conservative process can be related to $K(2)$ through

$$\beta_{\text{cons}} = 1 - K(2). \tag{10}$$

H can then be estimated simply given the field's spectral exponent combined with α and C_1 [using (5)] with $K(2)$:

$$H = \frac{\beta - \beta_{\text{cons}}}{2}$$
$$= \frac{\beta - 1}{2} + \left(\frac{C_1}{\alpha - 1}\right)(2^{\alpha-1} - 1). \tag{11}$$

Table I shows that the estimated values of H are slightly negative (≈ -0.15 depending somewhat on the wavelength and polarization) indicating that a small amount of fractional differentiation is required to recover the observed from the corresponding conserved field.

VII. CONCLUSION

Due to nonlinear ice dynamics, sea-ice has complex, highly variable structures spanning wide ranges of scale. Since there is no characteristic length in these processes, we expect the dynamically significant ice fields to be universal multifractals over wide ranges of scale. Using several new data analysis techniques—notably the Double Trace Moment technique designed especially for this purpose—we estimate the universal

parameters $\alpha \approx 1.85 \pm 0.05$, $C_1 \approx 0.0086 \pm 0.0041$, $H \approx -0.15 \pm 0.05$, on SAR data at L and C-band frequencies for three polarizations and for two scenes. The scene by scene comparison indicates that the estimates are (within statistical accuracy) independent of the scene. The wavelength and polarization comparison indicates no significant wavelength variations, with only small polarization variations; the HV polarization seems to have a value of H systematically greater than the other polarizations and, the values of C_1 for HH and VV are similar but differ to the values for the HV polarization, for both scenes, although the effect is barely detectable with just two scenes. The scaling in the HV channel is also systematically better; the other polarizations exhibit a slight dip in the spectrum at wavenumbers corresponding to around 50 m.

The physics of the different polarizations explains why the HV is somewhat different. Whereas the HH and VV polarizations represent more the surface characteristics, the HV polarization is a second-order scattered field representing a volumetric response to dielectric fluctuations of similar scales. This is a direct response to the fluctuation of the dielectric tensor, and represents some anisotropy in the sea-ice relating back to the predominant crystallography and brine-inclusion structure (within the crystal lattice of the sea-ice).

The analysis reported here concerns the scattering amplitude field; perhaps the most significant direct inference about the dynamics is that they are likely to be scaling over the corresponding range of sizes since—due to the nonlinear relations between the different fields—a break in the scaling of the dynamics will be reflected in the scaling of the amplitude fields. It is possible however that more quantitative inferences about the ice field can be made, since recent results from the simpler scalar radar multifractal observer's problem [21], [42] indicate that the radar scattering coefficient is likely to have the same basic multifractal parameters as the underlying cross-section field (i.e., the "speckle" doesn't change the basic multifractal indices α, C_1, only H). These results already permit multifractal simulations of ice scattering amplitudes using techniques used by [38] (although the anisotropy generator must be estimated in order to obtain realistic texture) and will provide statistical constraints on dynamical models of ice. The relations between the results at different wavelengths and polarizations will next be investigated in more detail with the help of Lie cascades [36].

REFERENCES

[1] D. Schertzer and S. Lovejoy, "Generalized scale invariance in turbulent phenomena," *Physico-Chem. Hydrodyn. J.*, vol. 6, pp. 623–635, 1985.
[2] S. Lovejoy, D. Schertzer, and A. A. Tsonis, "Functional box-counting and multiple elliptical dimensions in rain," *Science*, vol. 235, pp. 1036–1038, 1987.
[3] S. Lovejoy and D. Schertzer, "Multifractals, universality classes, satellite and radar measurements of clouds and rain," *J. Geophys. Res.*, vol. 95, pp. 2021–2034, 1990.
[4] D. Lavallée and D. Jourdan, "Universal multifractal properties of microwave satellite data," in *Proc. ASPRS/ACSM*, A. J. Lewis and G. G. Kelly, Eds., New Orleans, LA, 1993, pp. 171–181.
[5] Y. Tessier, S. Lovejoy, and D. Schertzer, "Universal multifractal: Theory and observations for rain and clouds," *J. Appl. Meteor.*, vol. 32, pp. 223–250, 1993.

[6] B. R. Kerman, "A multifractal equivalent of the Beaufort scale for sea-state," *Geophy. Res. Lett.*, vol. 20, pp. 297–300, 1993.
[7] B. R. Kerman and L. Bernier, "A multifractal representation of breaking waves on the ocean surface," *J. Geophys. Res.*, vol. 99, pp. 16179–16196, 1994.
[8] C. K. Meneveau and R. Sreenivasan, "Simple multifractal cascade model for fully developed turbulence," *Phys. Rev. Lett.*, vol. 59, pp. 1424–1427, 1987.
[9] F. Schmitt, D. Lavallée, D. Schertzer, and S. Lovejoy, "Empirical determination of universal multifractal exponents in turbulent velocity fields," *Phys. Rev. Lett.*, vol. 68, pp. 305–308, 1992.
[10] S. Lovejoy and D. Schertzer, "Our multifractal atmosphere: A unique laboratory for nonlinear dynamics," *Phys. Canada*, vol. 46, no. 4, pp. 62–71, 1990.
[11] D. Lavallée, S. Lovejoy, D. Schertzer, and P. Ladoy, "Nonlinear variability and landscape topography: Analysis and simulation," in *Fractals in Geography*, L. De Cola and N. Lam, Eds. Englewood Cliffs, NJ: Prentice-Hall, 1993, pp. 158–192.
[12] C. Hooge, S. Lovejoy, D. Schertzer, F. Schmitt, and J. F. Malouin, "Multifractal phase transitions: The origin of self-organized criticality in earthquakes," *Nonlinear Proc. Geophys.*, vol. 1, pp. 191–197, 1994.
[13] D. Schertzer and S. Lovejoy, "Standard and advanced multifractal techniques for remote sensing," in *Fractals in Geoscience and Remote Sensing*, G. Wilkinson, I. Kanellopoulos, and J. Mégier, Eds., Image Understanding Research Series, vol. 1. Luxembourg: Office Official Publ. European Commun., 1995, pp. 11–40.
[14] S. Lovejoy and D. Schertzer, "How bright is the coast of Brittany?" in *Fractals in Geoscience and Remote Sensing*, G. Wilkinson, I. Kanellopoulos, and J. Mégier, Eds., Image Understanding Research Series vol. 1. Luxembourg: Office Official Publ. European Commun., 1995, pp. 102–151.
[15] D. A. Rothrock and A. S. Thorndike, "Geometric properties of the underside of sea-ice," *J. Geophys. Res.*, vol. 85, pp. 3955–3963, 1980.
[16] J. Key and A. S. McLaren, "Fractal nature of the sea-ice draft profile," *Geophys. Res. Lett.*, vol. 18, pp. 1437–1440, 1991.
[17] G. C. Bishop and S. E. Chellis, "Fractal dimension: A descriptor of ice keel surface roughness," *Geophys. Res. Lett.*, vol. 16, no. 9, pp. 1007–1010, 1989.
[18] M. R. Drinkwater, "Multi-frequency imaging radar polarimetry of sea ice," in *Ice Technology for Polar Operations*, T. K. S. Murthy, J. G. Paren, W. M. Sackinger, and P. Wadhams, Eds. Southampton: Comput. Mech. Publ., 1990, pp. 365–376.
[19] M. R. Drinkwater, R. Kwok, D. P. Winebrenner, and E. Rignot, "Multi-frequency polarimetric SAR observations of sea ice," *J. Geophys. Res.*, vol. 96, no. C11, pp. 20679–20698, 1991.
[20] M. R. Drinkwater, R. Kwok, E. Rignot, H. Israelsson, R. O. Onstott, and D. P. Winebrenner, "Potential applications of polarimetry to the classification of sea ice," in *Microwave Remote Sensing of Sea Ice*, F. D. Carsey, Ed., Geophysical Monograph 28. Wash., DC: Amer. Geophys. Union, 1992, ch. 24, pp. 419–430.
[21] M. Duncan, "Analysis and simulation of radar reflectivities of rain with universal multifractals," Ph.D. dissertation, McGill Univ., Canada, p. 205, 1993.
[22] P. F. Fougere, "On the extreme accuracy of maximum entropy spectrum estimation from an error-free autocorrelation function," in *IEEE Proc. Int. Conf. Acoustics, Speech and Signal Processing*, Piscataway, NJ, 1987, pp. 352–355.
[23] D. Schertzer and S. Lovejoy, "Physical modeling and analysis of rain and clouds by anisotropic scaling multiplicative processes," *J. Geophy. Res.*, vol. 92, pp. 9693–9714, 1987.
[24] _____, "Nonlinear geodynamical variability: Multiple singularities, universality and observables," in *Scaling, Fractals and Non-Linear Variability in Geophysics*, D. Schertzer and S. Lovejoy, Eds. Norwell, MA: Kluwer, 1991, pp. 41–82.
[25] K. Pflug, S. Lovejoy, and D. Schertzer, "Generalized scale invariance, differential rotation and cloud texture," in *Nonlinear Dynamics of Structures*, R. Z. Sagdeev, U. Frisch, F. Hussain, S. S. Moiseev, and N. S. Erokhin, Eds. Singapore: World Scientific, 1991, pp. 71–80.
[26] G. Lewis, "The scale invariant generator technique and scaling anisotropy in geophysics," M.Sc. thesis, McGill Univ., Canada, 1993.
[27] R. T. Austin, A. W. England, and G. H. Wakefield, "Special problems in the estimation of power-law spectra as applied to topographical modeling," *IEEE Trans. Geosci. Remote Sensing*, vol. 32, no. 4, pp. 928–939, 1994.
[28] G. Parisi and U. Frisch, "A multifractal model of intermittency," in *Turbulence and Predictability in Geophysical Fluid Dynamics and Climate Dynamics*, M. Ghil, R. Benzi, and G. Parisi, Eds. Amsterdam: North-Holland, 1985, pp. 84–88.

[29] D. Schertzer and S. Lovejoy, "Nonlinear variability in geophysics: Multifractal analysis and simulations," in *Fractals: Their Physical Origins and Properties,* Pietronero, Ed. New York: Plenum, 1989, pp. 49–79.
[30] D. Schertzer, S. Lovejoy, and F. Schmitt, "Structures in turbulence and multifractal universality," in *Small-Scale Structures in 3D and MHD Turbulence,* M. Meneguzzi, A. Pouquet, and P. L. Sulem, Eds. New York: Springer-Verlag, 1995, pp. 137–144.
[31] P. Brax and R. Pechanski, "Levy stable law description on intermittent behavior and quark-gluon phase transitions," *Phys. Lett. B,* vol. 253, pp. 225–230, 1991.
[32] S. Kida, "Log stable distribution and intermittency of turbulence," *J. Phys. Soc. Japan,* vol. 60, pp. 5–8, 1991.
[33] D. Lavallée, "Multifractal analysis and simulation techniques and turbulent fields," Ph.D. dissertation, McGill Univ., Canada, p. 142, 1991.
[34] D. Schertzer and S. Lovejoy, "Hard and soft multifractal processes," *Physica A,* vol. 185, pp. 187–194, 1992.
[35] _____, "Multifractal generation of self-organized criticality," in *Fractals in the Natural and Applied Sciences,* M. M. Novak, Ed. Amsterdam: IFIP, 1994, pp. 325–339.
[36] D. Schertzer, S. Lovejoy, and D. Lavallée, "Generic multifractal phase transitions and self-organized criticality," in *Cellular Automata: Prospects in Astrophysical Applications,* J. M. Perdang and A. Lejeune, Eds. Singapore: World Scientific, 1993, pp. 216–227.
[37] M. Ostoja-Starjewski, "Micromechanics as a basis of stochastic finite elements and differences: An overview, in mechanics Pan-America," in *Appl. Mech. Rev.,* M. R. M. Crespo da Silva and C. E. N. Mazzilli, Eds., 1993, vol. 46, pp. S136–S143.
[38] S. Pecknold, S. Lovejoy, D. Schertzer, C. Hooge, and J. F. Malouin, "The simulation of universal multifractals," in *Cellular Automata: Prospects in Astrophysical Applications,* J. M. Perdang and A. Lejeune, Eds. Singapore: World Scientific, 1993, pp. 228–267.
[39] D. Schertzer and S. Lovejoy, "From scalar cascades to Lie cascades: Joint multifractal analysis of rain and cloud processes," in *Space/Time Variability and Interdependencies in Hydrological Processes,* R. A. Feddes, Ed. Cambridge: Cambridge Univ. Press, 1995, pp. 153–173.
[40] _____, "The multifractal phase transition route to self-organized criticality in turbulence and other dissipative nonlinear systems," *Phys. Rep.,* 1996, in press.
[41] C. E. Livingstone and M. R. Drinkwater, "Springtime C-band SAR backscatter signatures of labrador sea marginal ice: Measurements versus modeling predictions," *IEEE Trans. Geosci. Remote Sensing,* vol. 29, pp. 29–41, 1991.
[42] S. Lovejoy, M. Duncan, D. Schertzer, "The scalar multifractal radar observer's problem," *J. Geophys. Res.,* to be published.
[43] A. S. Monin and A. M. Yaglom, *Statistical fluid mechanics: Mechanics of turbulence.* Cambridge, MA: The MIT Press, vol. 1, 1971, pp. 205–249.
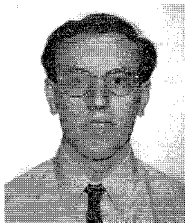
Tony Falco received the B.Sc. degree in physics (1993) and the M.Sc. degree in medical physics (1996), both from McGill University, Québec, Canada.

He is presently pursing a Ph.D. degree in physics at McGill University with specialization in medical physics. His doctoral thesis focuses on studying and improving the efficiency of a prototype low-dose, amorphous Selenium-based, therapy imaging detector, which he helped to develop. His research interests include image processing as well as absolute efficiency estimation, spectral analysis, and structural recognition in radiation detector acquired images.

Mr. Falco is a member of both the Canadian Organization of Medical Physicists (COMP) and the American Association of Physicists in Medicine (AAPM).

Frédéric Francis received the B.Sc. degree in physics from McGill University, Québec, Canada.

He is currently Director of Technology at Lateral Logic, which specializes in real-time visual simulations for use in personnel training and machine prototyping. His work includes developing and implementing physically accurate models of industrial processes and natural phenomena. His research interests include the visualization and simulation of geophysical data as well as virtual environments and neural networks.

Shaun Lovejoy received the B.A. and M.A. degrees in theoretical physics from Trinity College, Cambridge, England (1976 and 1981) and the Ph.D. degree in physics from McGill University, Québec, Canada (1981). The title of his Ph.D. dissertation was "The Remote Sensing of Rain."

He was an Assistant Professor (1985) and Associate Professor (1990) of physics at McGill University. He is the Co-editor of the European Geophysical Society Journal *Nonlinear Processes in Geophysics.* He has worked in the area of fractals and multifractals since 1979, especially with applications in geophysics, turbulence, and remote sensing. Highlights include multifractals (1983), generalized scale invariance (1983–1985), universal multifractals (1987), the codimension formalism for multifractals (1987), continuous cascade processes (1987), vector and tensor multifractal processes (1993), and the multifractal phase transition route to self-organized criticality (1993).

Daniel Schertzer, photograph and biography not available at the time of publication.

Bryan Kerman, photograph and biography not available at the time of publication.

Mark Drinkwater received the B.Sc. (Hons) degree in geography from Durham University, England, in 1984, specializing in remote sensing in glaciology. He was awarded a Council of Europe Diploma in Remote Sensing in Engineering from the University of Dundee in 1984; and the Ph.D. degree in geophysics for a thesis on radar remote sensing of polar ice, from the Scott Polar Research Institute and Emmanuel College, of the University of Cambridge, England, in 1988.

During 1987-1988 he worked as a Research Scientist for Polar Oceans Associates, a U.K. division of Science Applications Inc. of San Diego, CA, before joining the Jet Propulsion Laboratory, California Institute of Technology, Pasadena, CA, in April 1988. At JPL, he has studied techniques in modelling microwave backscatter behavior and the geophysics of snow and sea-ice media. His recent interests have included airborne and space shuttle multifrequency polarimetric microwave observations of sea ice and terrestrial ice sheets. His current work is in the development of techniques combining geophysical models with information extracted from satellite microwave data, for the estimation of surface fluxes of heat and salt in the polar oceans. Presently, he is an Associate Editor of the *Journal of Geophysical Research Oceans.*

Dr. Drinkwater is a member of the International Glaciological Society, the American Geophysical Union, the IEEE, the Oceanography Society and in 1989 was elected to the Electromagnetics Academy. In 1990 he was presented with an IEEE Prize Paper Award for a manuscript on radar polarimetry of sea ice.photograph and biography not available at the time of publication.